

BACKSCATTERING TOPOGRAPHY OF LARGE, NEARLY PERFECT QUARTZ CRYSTALS

Many synchrotron radiation beamlines that produce hard X-rays use optical elements made from perfect crystals of silicon. However, silicon is limited in certain ways by its highly symmetric cubic lattice structure. Quartz, with a non-centrosymmetric trigonal lattice, has shown potential, especially for inelastic X-ray scattering (IXS) energy analyzers. These must provide not only good energy resolution, but also large angular acceptance and large area for efficient collection of the low and diffuse scattered flux. Large perfect silicon wafers oriented to Bragg reflections near backscattering ($\theta_B \approx 90^\circ$) have fulfilled these needs, but large perfect quartz wafers, if available, would make IXS feasible under a wider range of conditions [1]. While no silicon backscattering reflection below 12 keV offers a bandpass below 9 meV, quartz can go as low as 1 meV, making phonon measurements feasible at lower energies. Quartz also offers backscattering reflections at 184 distinct energies for photons of 5-12 keV, while silicon offers them at only 22. Absorption and emission spectroscopy and nuclear resonant scattering, which require a photon beam of specific energy, benefit from this.

Large-area measurements are needed to find out whether obtainable quartz wafers are indeed good enough. Backscattering from quartz has been investigated with a small-area beam [2], but not with the large-area beams needed for a topograph. Non-backscattering topographic images of quartz also exist [3] but may be outdated and do not show whether the energy resolution requirements for IXS are fulfilled. Therefore, both topographic images and reflectivity scans of two quartz wafers have been made using the (7 -4 -3 4) reflection of 9.979 keV photons ($\theta_B = 89.77^\circ$, Darwin width 2.0 meV). These "A grade" wafers are 40 mm in diameter, 2.0 mm thick, and are polished on both sides.

The measurements were performed at beamline BL29XU. A high-resolution monochromator with a calculated bandpass of 1.91 meV, built using the design in [4], was placed downstream of the inbuilt high-heat load monochromator, but still near the source.

The quartz wafers were placed in the 1-km hutch because the beam size increases many times over this distance. Reflectivity curves as a function of photon energy were made using an APD; topographic

images were recorded on a CCD camera using an $8 \times 8 \text{ mm}^2$ beam.

The image in Fig. 1(a) is a composition of topographs covering most of the first quartz wafer. It shows both a distinctly reduced reflectivity in the lower left-hand side of the wafer and defects of smaller area scattered throughout the wafer. The graph in Fig. 1(b) shows two curves of reflectivity *versus* photon energy that

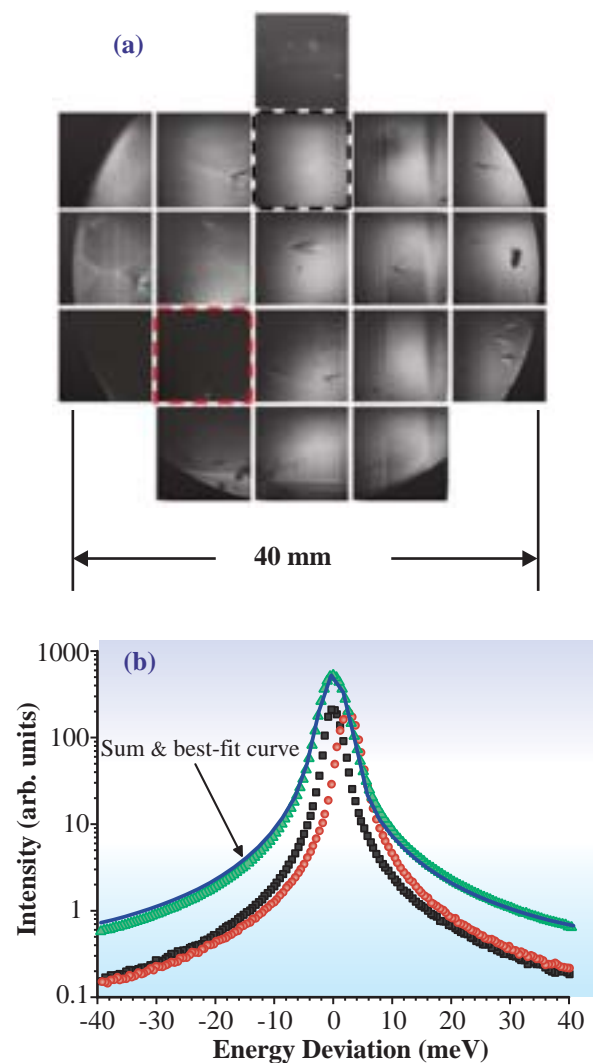


Fig. 1. (a) Topograph of quartz wafer. (b) Comparison of energy curves in two regions (outlined with corresponding colors at the top) and sum of energy curves over all regions. The best-fit curve to the sum is a Gaussian of FWHM 4.17 meV centered at +0.39 meV plus a Lorentzian of FWHM 3.64 meV centered at -0.48 meV. The peak amplitude of the Gaussian is 0.994 times that of the Lorentzian.

Instrumentation & Methodology

were measured at each region of the wafer. The peak widths of these curves lay between 2.9 and 4.0 meV. The reflectivity curves of the top and lower left-hand regions of the wafer are similar but are shifted by 2.5 meV, indicating a lattice spacing variation of $2.5 \text{ meV} / 9.979 \text{ keV} = 0.25 \text{ ppm}$. The same graph also shows the sum of the reflectivity curves over all the imaged regions. Properly accounting for temperature drifts, one finds a FWHM of 4.0 meV, which includes the resolution function of the high-resolution monochromator since no deconvolution was performed.

Figure 2 shows the $1 \times 1 \text{ mm}^2$ area around one

small defect of the second wafer with a defect-free region of the same wafer. The weaker and broader reflectivity curve at the defective region shows that its lattice structure is strongly distorted. The observed area density of these small defects was 2 per cm^2 in the first wafer and 5 per cm^2 in the second wafer.

In summary, nearly perfect large-area quartz wafers are commercially available. Low defect concentrations are found even over areas of 10 cm^2 , while reflectivity curves have shown a bandpass of 4.0 meV. Quartz thus shows great promise as a material for IXS analyzers and other X-ray optical elements.

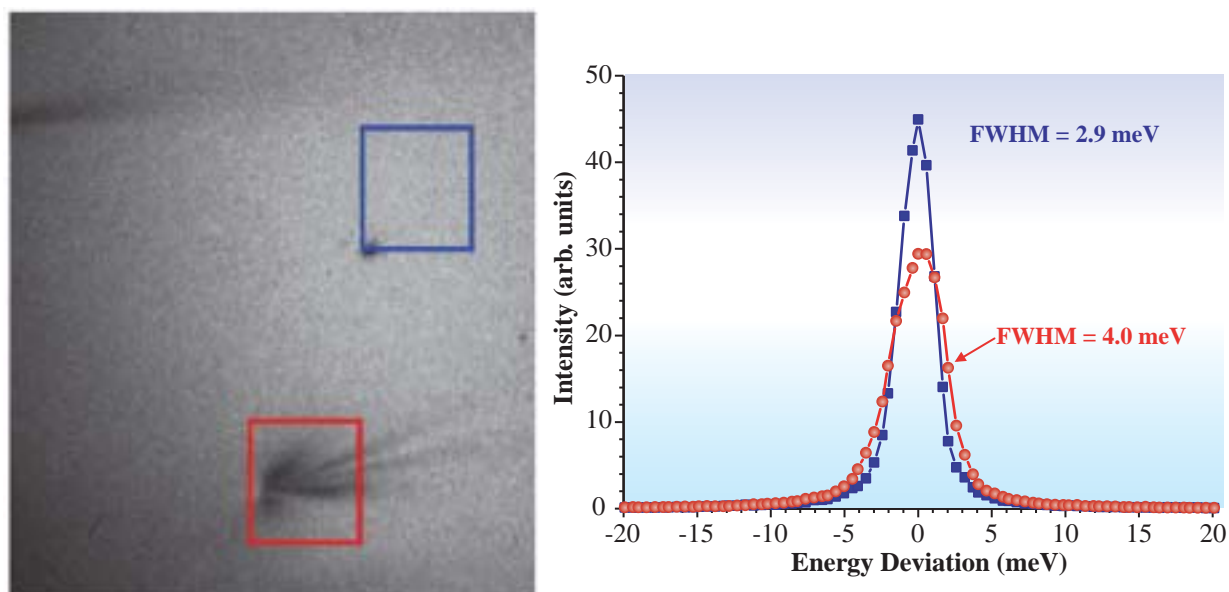


Fig. 2. Comparison of defective and defect-free areas of quartz wafer. For details, see text.

John P. Sutter^{a,*†}, Alfred Q.R. Baron^b and Tetsuya Ishikawa^{a,b}

^a SPring-8 / JASRI

^b SPring-8 / RIKEN

*E-mail: John.Sutter@diamond.ac.uk

† Present address: Diamond Light Source Ltd, Rutherford Appleton Laboratory, UK

References

- [1] J.P. Sutter, A.Q.R. Baron, T. Ishikawa and H. Yamazaki: *J. Phys. Chem. Solids* **66** (2005) 2306.
- [2] Y. Imai *et al.*: SPring-8 User Experiment Report No. 8 (2001) p. 70; No. 9 (2002) p. 74.
- [3] J. Yoshimura *et al.*: *J. Cryst. Growth* **46** (1979) 691.
- [4] M. Yabashi *et al.*: *Rev. Sci. Instrum.* **72** (2001) 4080.